Molecular Therapy
Methods & Clinical Development
Original Article

Targeted adenovirus-mediated transduction of human T cells *in vitro* and *in vivo*

Patrick C. Freitag,[1] Meike Kaulfuss,[2] Lea Flühler,[1] Juliane Mietz,[2] Fabian Weiss,[1] Dominik Brücher,[1,4] Jonas Kolibius,[1] K. Patricia Hartmann,[1] Sheena N. Smith,[1,4] Christian Münz,[3] Obinna Chijioke,[2] and Andreas Plückthun[1]

[1]Department of Biochemistry, University of Zurich, Winterthurerstrasse 190, 8057 Zurich, Switzerland; [2]Cellular Immunotherapy, Institute of Experimental Immunology, University of Zurich, Winterthurerstrasse 190, 8057 Zurich, Switzerland; [3]Viral Immunobiology, Institute of Experimental Immunology, University of Zurich, Winterthurerstrasse 190, 8057 Zurich, Switzerland

Clinical success in T cell therapy has stimulated widespread efforts to increase safety and potency and to extend this technology to solid tumors. Yet progress in cell therapy remains restricted by the limited payload capacity, specificity of target cell transduction, and transgenic gene expression efficiency of applied viral vectors. This renders complex reprogramming or direct *in vivo* applications difficult. Here, we developed a synergistic combination of trimeric adapter constructs enabling T cell-directed transduction by the human adenoviral vector serotype C5 *in vitro* and *in vivo*. Rationally chosen binding partners showed receptor-specific transduction of otherwise non-susceptible human T cells by exploiting activation stimuli. This platform remains compatible with high-capacity vectors for up to 37 kb DNA delivery, increasing payload capacity and safety because of the removal of all viral genes. Together, these findings provide a tool for targeted delivery of large payloads in T cells as a potential avenue to overcome current limitations of T cell therapy.

INTRODUCTION

Decades of research have aimed to genetically engineer T cells for scientific and therapeutic purposes.[1,2] Exceptional advances in cell therapy have been accomplished by using recombinant retrovirus vectors for *ex vivo* applications. Although adeno-associated viral vectors or non-viral delivery strategies have been applied to engineer T cells, so far only *ex vivo* retro- or lentiviral transduction achieved U.S. Food and Drug Administration (FDA) approval.[3–6] To circumvent viral production or the toxicity of foreign DNA delivery, various techniques, such as linear DNA transfection,[2,7] RNA transfection,[8] and RNA-containing lipid nanoparticles,[9] have been harnessed. Throughout this progress, gene constructs have also become increasingly complex, with growing numbers of proteins encoded.[10] However, current methods remain limited to only allow uptake of a very limited size range of DNA, thus rendering the combination of multiple genes or the delivery of large cargoes difficult and cumbersome.

The use of a single vector would be advantageous compared with multiple transduction or multi-step transfections to enable the delivery of all DNA components simultaneously with defined gene ratios in the transduced T cell resulting in a homogeneous effector cell population. Especially at low transduction efficiencies, multiple transduction steps bear the risk of uncontrolled ratios of transgenes in target cells potentially leading to heterogeneous expression of effector proteins, loss of optimal synergies or control mechanisms. The efficient delivery of large cargos to T cells might also enable potential *in vivo* applications, as additional safety features could be encoded such as suicide genes, cell type-specific gene expression control, and genetic feedback loops. However, *in vivo* applications require additional targeting and detargeting mechanisms to minimize nonspecific uptake by other cells leading to otherwise unknown side effects.[11] The ideal vector would thus combine large packaging capacity, effective transduction, high safety margin, and receptor-specific targeting and could then be universally applied for various *in vitro* and *in vivo* applications.

Human adenovirus serotype 5 vectors (HAdV-C5) can be consistently produced at high purity and have been validated in various clinical trials and animal models. Human adenovirus (HAdV) genomes localize episomally and extra-chromosomally, thus minimizing the risk for undesired insertional mutagenesis and germline transmission. Additionally, multiple generations of HAdV-C5-based vectors have been developed by deleting various genes from the adenoviral genome. Maximal packaging capacity ranges from 7 kb DNA (non-replicative, first-generation vectors) up to a cargo size of 37 kb, as it has been shown for high-capacity vectors (HC-AdVs). HC-AdVs are devoid of all viral genes, and this further increases their safety for potential human applications.[12–15] Demonstrating their versatility, HC-AdVs have been reported as a single delivery vehicle containing both donor DNA and a Cas9 system for site-specific insertion and deletion.[16] Thus, HAdV-C5 qualifies as an ideal vector to overcome current limitations in T cell engineering methods.

Natural cellular entry of HAdV-C5 vectors is mediated through contact of the homotrimeric fiber-knob protein with the coxsackie and adenovirus receptor (CAR) and subsequent interaction of the penton

Received 21 November 2022; accepted 22 February 2023;
https://doi.org/10.1016/j.omtm.2023.02.012.

[4]Present address: Vector BioPharma AG, Aeschenvorstadt 36, 4051 Basel, Switzerland

Correspondence: Andreas Plückthun, Department of Biochemistry, University of Zurich, Winterthurerstrasse 190, 8057 Zurich, Switzerland.
E-mail: plueckthun@bioc.uzh.ch

base RGD-motif with $\alpha_v\beta_3$- or $\alpha_v\beta_5$-integrins on the cell membrane.[17] Both CAR and RGD-binding integrins are absent in human T cells.[18–21] Therefore, T cells are difficult to transduce by HAdV-C5 without modifying either the vector or the cell.[18–21] This has led to the engineering of T cells expressing either CAR[22] or $\alpha_V\beta_{3/5}$ integrins,[20] making the cells susceptible to adenoviral infection. However, alterations in T cells are laborious and unfeasible for clinical applications and interference with the T cell gene expression pattern would influence possible outcomes in mechanistic studies to guide clinical applications. As an alternative, the generation of chimeric adenoviral vectors such as Ad5/35 have been reported to transduce T cells. These chimeric vectors, however, bind to CD46, which is expressed on all nucleated human cells, which renders their tropism broadly specific, potentially hampering *in vivo* applications and payload design.[23,24] Furthermore, an improvement of the Ad5/35 for primary cell transduction has been described by inserting the highly positively charged protein transduction domain of the HIV-1 Tat protein into the hypervariable region 5 of the hexon in the adenoviral vector.[25] Although increased transduction of human T cells was measured *in vitro*, the exact receptor interaction remains unclear and an increased transduction *in vitro* was also measured in multiple cell types such as macrophages, pancreatic cells, prostate cancer cells, and glioma cells.[25]

We hypothesized that our previously described and *in vivo* validated trimeric adapter technology,[26–28] could be amended to be an easily applicable method enabling targeted HAdV-C5-mediated transduction of T cells. Compared with other serotypes or capsid-engineered adenoviral vectors, T cell transduction by HAdV-C5 vectors would use the most commonly used adenoviral vector[11] which was characterized in various research and clinical settings. Briefly, a bispecific adapter blocks the natural tropism of HAdV-C5 by binding to the fiber-knob through a designed ankyrin repeat protein (DARPin) while redirecting specificity to the chosen cell-surface biomarker by a retargeting moiety.[27] This is achieved by a C-terminally fused trimerization module, allowing the DARPin to bind the trimeric fiber-knob as a clamp, which leads to an extremely stable binding interaction without any detectable off rate.[27] Additionally, *in vivo* applications become feasible because of the compatibility with our previously reported adenovirus capsid-covering shield.[29] This shield is based on a trimerized anti-capsid antibody fragment that is combined with capsid mutations, resulting in increased tissue specificity by reducing liver uptake and reducing access to antibodies.[29] Together, this technology has been termed shielded retargeted adenovirus (SHREAD).[15,26–31] Here we report efficient transduction of activated and non-activated human T cells *in vitro* and show transgene expression in human T cells *in vivo* using such a retargeted HAdV-C5. Our adapter-mediated T cell transduction could be explored to reprogram a patient's T cell repertoire for more efficient and safe recognition of tumor and infectious disease antigens.

RESULTS

Combinatorial adapters efficiently mediate transduction of human T cells

Although transduction of human primary T cells has been challenging using HAdV-C5, the T lymphocyte cancer cell line Jurkat E6 shows vastly improved uptake over primary T cells (Figure S1), as has been reported by others.[32] We hypothesized that this increase in HAdV-C5 susceptibility is due to the replicative state of this cancerous cell line in contrast to resting primary T cells. To test this hypothesis, we compared the transduction efficiency of peripheral blood mononuclear cells (PBMCs) with and without prior activation using untargeted HAdV-C5 (U/AdV), which is not bound to any retargeting adapter. Indeed, an increase of 4.9-fold in T cell transduction with U/AdV was observed after stimulation of cells with magnetic beads containing both anti-CD3 as well as anti-CD28 antibodies (anti-CD3/CD28 beads) (Figure S2).

Therefore, we aimed to directly couple T cell activation to HAdV-C5 binding to generate effective and targeted transduction. We generated three different adapter proteins to the membrane proteins CD3, CD28, and the IL-2 receptor, which are all expressed on T cells (Figure 1A). Each of these adapters is homotrimeric, and they are applied as a mixture to the virus, thus stochastically populating the 12 fiber knobs of the virion leading to a multispecific targeted virion. We designed single-chain variable fragments (scFvs) from the humanized anti-CD3 antibody V9[33,34] and the humanized anti-CD28 antibody TGN1412,[35] and we implemented the natural ligand human IL-2 as the targeting domain for IL-2R in our three adapter designs. The proteins were expressed in mammalian cells and their purity was confirmed using reducing SDS-PAGE and size exclusion chromatography (SEC) high-performance liquid chromatography (HPLC) analysis (Figures S3A and S3B).

As a first proof-of-concept experiment, we covered the 12 fiber knobs of first-generation HAdV-C5 vectors encoding infrared fluorescent protein (iRFP670). The virions were covered with each single adapter independently, or with a 1:1:1 combination of all three adapters (combination retargeted adenoviral vector [Comb.R/AdV]) while keeping the total molar amount of the sum of all adapters constant. As we did not alter the knob-binding domain of our adapters, we expect equal binding affinities to the fiber knob. Assuming equal distribution, this predicts that 98% of vectors carry at least one copy of each adapter, resulting in multispecific retargeted adenoviral vectors.

Activated PBMCs from three separate donors were then transduced overnight, and reporter expression was analyzed 48 h after transduction. All single-agent adapters improved transduction efficiency in $CD3^+$ T cells (25%–53%) (Figure 1B). However, the combination of adapters yielded additive or even synergistic effects and achieved transgene expression in up to 76% of $CD3^+$ T cells, showcasing the efficiency of a rationally designed multispecific targeting strategy for hard-to-transduce cells (Figure 1B). U/AdVs not covered with retargeting adapters are not directed to T lymphocytes and achieved transgene expression in only a comparably small fraction (15%) of pre-activated T cells (Figure 1B).

Next, we investigated the influence of different combinations and molar ratios of adapters on transduction efficiencies in non-activated T cells (Figure 1C). All conditions tested enhanced the transduction

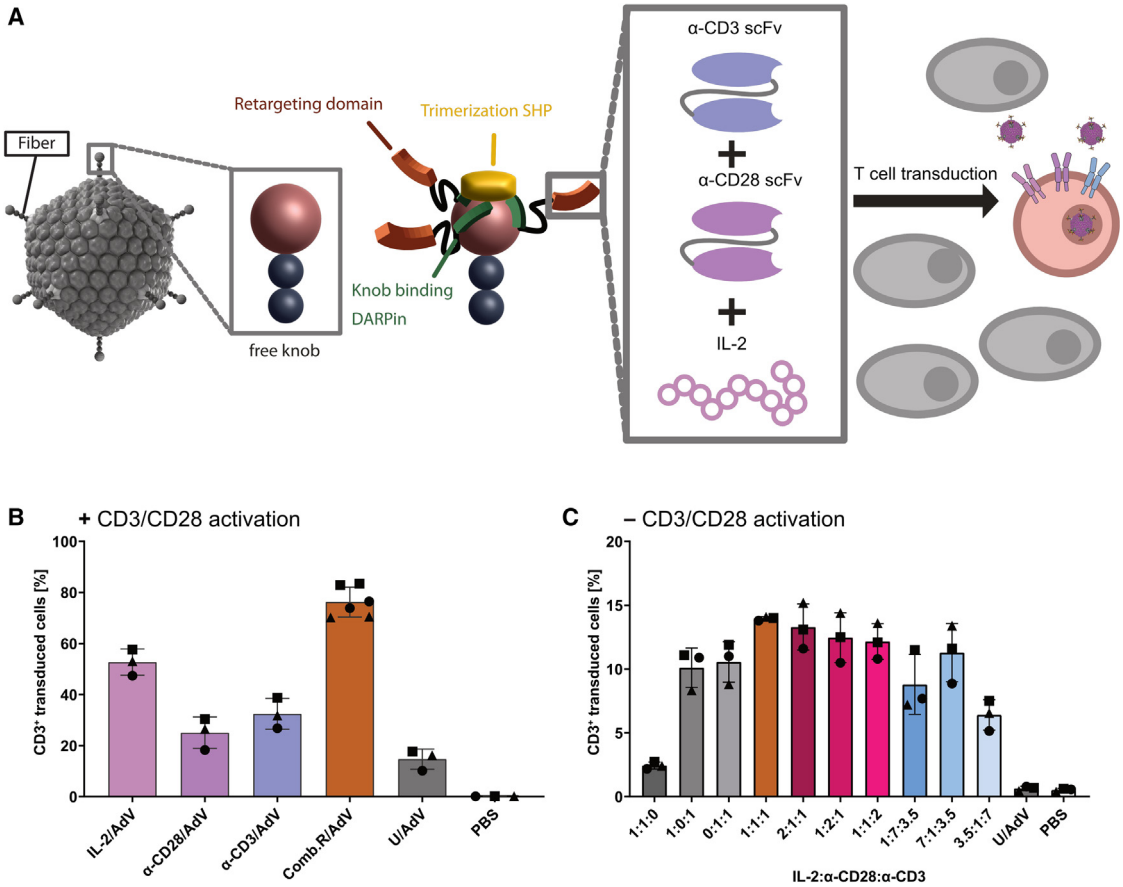

Figure 1. Primary human T cells are efficiently transduced by HAdV-C5 by using a combination of adapters targeting CD3, CD28, and IL-2 receptor

(A) Schematic outline of the adapter system used to create receptor-specific transduction. The HAdV-C5 fiber knob (left) is bound by a trimeric adapter protein consisting of three domains: the retargeting domain (orange), the trimerization domain (yellow), and the knob binding DARPin (green). We implemented three different molecules as a retargeting domain (anti-CD3 scFv, anti-CD28 scFv, and IL-2) and used their mixture for receptor-specific T cells targeting (right), occupying the 12 knobs on a virion in a stochastic manner. For inhibition of liver uptake *in vivo*, an additional shield protein (a trimerized anti-hexon scFv, purple, right virus picture) is added to cover the hexon protein of the HAdV-C5. SHP, capsid-stabilizing protein of lambdoid phage 21; scFv, single-chain variable fragment. (B) Quantification of transduction efficiency on pre-activated PBMCs using HAdV-C5 retargeted with single adapters (IL-2, α-CD28, and α-CD3), a 1:1:1 combination of these three adapters (Comb.R/AdV), untargeted vectors (U/AdV) using no adapter, or a PBS control. Whenever adapters were used, the total ratio of adapter/knob is kept constant at 32.5:1. (C) Flow cytometry analysis of the transduction efficiency on T cells using different ratios of adapters (IL-2:α-CD28:α-CD3) on non-pre-activated PBMCs, while maintaining constant total adapter/knob ratios. Individual symbols represent single donors, repeated transductions using the same donor are indicated by addition of the same symbol. Data are shown as mean ± SD.

efficiency compared with untargeted vectors, yet a 1:1:1 ratio of IL-2 to α-CD28 to α-CD3 adapters yielded the highest transduction rate (14%). In contrast, transduction with the untargeted vector with a rate of 0.6% remained in the range of the non-transduced control (0.5%), underlining the importance of rationally chosen adapters for HAdV-C5-mediated DNA delivery into non-activated T cells. Interestingly, the absence of one of these three adapters led to a reduction of transduction efficiency between 3% and 12%, which is in line with our previous data, suggesting additive effects of multispecific targeting. Intriguingly, even though studies involving anti-CD3 and anti-CD28 coated beads have suggested improved activation using a higher anti-CD28 ratio,[36] we did not observe an improvement in transduction efficiency by changing the adapter ratio away from 1:1:1 (Figure 1C). Presumably, changing the ratio from 1:1:1 would increase the subset of coated virions lacking at least one adapter, which could in turn potentially counteract synergistic effects of multispecific interactions. Taken together, our combination of adapters improved T cell transduction with and without prior activation of T cells.

Adapters successfully activate human T cells while increasing adenoviral transduction

As our combinatorial adapter design targeting different T cell activation pathways was implemented to increase the susceptibility of T cells to transduction, we next assessed if our adapter constructs indeed induce measurable T cell activation, and we explored correlations between adapter-mediated T cell activation and transduction of T cells.

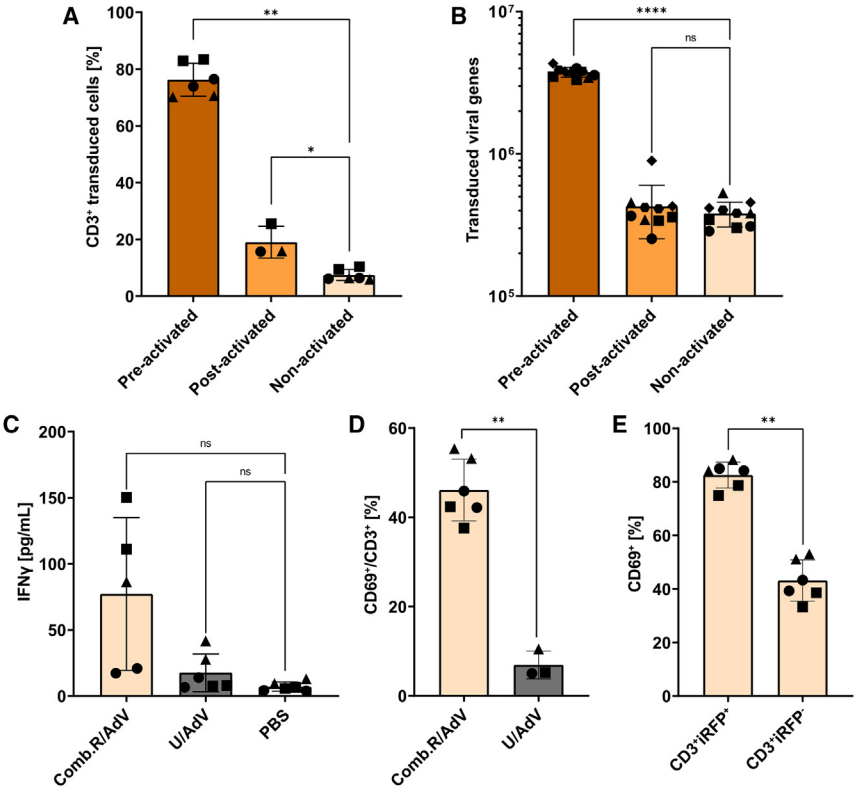

Figure 2. Influence of activation status in transduction of human T cells using Comb.R/AdV

(A) PBMCs were activated prior to transduction (pre-activated) or after transduction (post-activated) or did not receive a CD3/CD28 activation stimulus. Transduction efficiency was measured 48 h post-transduction (n = 3 independent donors; *p = 0.0443 and **p = 0.0022, determined using one-way ANOVA with Dunnett's test for multiple comparisons). (B) qPCR analysis seventy-two hours after transducing 50,000 pre-activated, post-activated, or non-activated PBMCs. Transducing units of Comb.R/AdVs (1.2×10^7) were used; each symbol represents the average of a technical duplicate (n = 5 independent donors; ****p < 0.0001; ns, p = 0.8326, determined using one-way ANOVA with Dunnett's test for multiple comparisons). (C) IFN-γ secretion of non-pre-activated PBMCs 48 h post-transduction by Comb.R/AdVs, U/AdVs, or PBS (n = 3 independent donors; ns, p = 0.0722, Comb.R/AdV to PBS; ns, p = 0.8523, determined using one-way ANOVA with Dunnett's test for multiple comparisons). (D) Flow cytometry analysis of CD69 expression on non-activated T cells 48 h post incubation with either Comb.R/AdV or U/AdV (n = 3 independent donors; **p = 0.0044, determined using two-tailed paired t tests). (E) CD69 expression of transduced (iRFP$^+$) or non-transduced (iRFP$^-$) T cells of non-activated Comb.R/AdV transduced PBMCs (transduction data a) (n = 3 independent donors; **p = 0.0048, determined using two-tailed paired t tests) Individual symbols represent single donors, repeated transductions using the same donor are indicated by addition of the same symbol. Data are shown as mean ± SD.

First, we determined whether T cell activation plays a major role during the cellular entry of viral vectors or at a later stage of host cell infection. For this purpose, PBMCs were transduced using Comb.R/AdV at different activation time points: PBMCs were either activated by anti-CD3/CD28 stimulation prior to transduction (pre-activated), directly after removal of virions from the medium (post-activated), or transduced without activation (Figure 2A). Although post-activation of T cells yielded an increase in transduction efficiency compared with the non-activated control, pre-activated cells remained distinctly more susceptible for adenoviral vector uptake. These data suggest that the yield-limiting steps of adenoviral vector transduction of T cells are involved in the actual cellular uptake of viral vectors, rather than in subsequent steps such as DNA delivery into the nucleus or transgene expression. To confirm this hypothesis, we conducted additional experiments in which we performed qPCR analysis to measure successful DNA delivery rather than expression of transgene (Figure 2B). For this purpose, 50,000 PBMCs were transduced with 1.2×10^7 transducing units Comb.R/AdV. We observed a 10-fold increase of viral DNA delivery if the PBMCs received activation signals prior to transduction compared with post-transduction or without any activation stimuli. In pre-activated cells, 3.8×10^6 viral genomes were detected, which represent 31% of the total applied transducing units as measured by natural transduction (in the absence of adapter) of the model cell line A549.

Having shown T cell transduction using our retargeting adapters, we assessed whether these constructs bound to the knobs of HAdV-C5 are able to directly activate T lymphocytes and if there is a correlation between activation marker expression and efficiency of transduction by retargeted HAdV-C5. To this end, we investigated secretion of IFN-γ and expression of the early activation marker CD69 upon transduction with Comb.R/AdV (Figures 2C and 2D). Indeed, the activation mediated by Comb.R/AdV was validated by induction of expression of the early activation marker CD69. Only a small fraction of T cells expressed CD69 after incubation with U/AdVs (7%), whereas almost half of all T cells (47%) expressed CD69 when incubated with the vector that was coated with retargeting adapters (Figure 2D). Additionally, a minor but non-significant increase in IFN-γ secretion was measured using Comb.R/AdV, although we see large variability between donors (Figure 2C). Together, these data show effective T cell stimulation by Comb.R/AdV induced by the adapters, which was expected, as synergistic effects of activation using anti-CD3 and anti-CD28 antibodies in combination of IL-2 are well described in the literature.[37] Furthermore, we found a correlation between CD69 expression and transduction susceptibility in non-activated T cells. After incubation with retargeted HAdV-C5 (Comb.R/AdV), we observed a stronger increase of CD69 expression in transduced T cells (83%) in contrast to non-transduced T cells (43%) (Figure 2E). Taken together, we highlight the importance of pre-activation by correlation of CD69 expression to Comb.R/AdV

transduction and confirmed the activating potential of Comb.R/AdV compared with untargeted vectors, supporting our rationale for the adapter design.

Adapter-mediated transduction remains target-dependent and specific

For direct application in mixed cell populations as found *in vivo*, we assessed the specificity of adapter-mediated transduction, as nonspecific uptake of adenoviral vectors has been recognized as a major hurdle for broad *in vivo* application.[11] To exclude nonspecific mechanisms such as hydrophobic interactions or other target receptor-independent endocytosis (e.g., caused by aggregation), we compared untargeted vectors (U/AdV) with blocked vectors. Blocked adenoviral vectors are bound by an adapter using the stable non-binding consensus DARPin E2_5 as a retargeting module (B/AdV).[38] Quantification by flow cytometry revealed iRFP expression in 15% of pre-activated T cells (U/AdV) compared with only 2% when blocked by non-binding adapters (Figure 3A). This reduced transduction efficiency implies that the uptake by T cells using Comb.R/AdV was indeed conferred by the specificity of the retargeting module and was not due to nonspecific interaction caused by the general adapter design. Conversely, the transduction of T cells using untargeted HAdV-C5 is higher than with the non-binding adapters, implying that T cell transduction is facilitated by the fiber-knob protein of the virion. To the best of our knowledge, an interaction of the HAdV-C5 knob with human T cells has previously not been described and was thought to be absent because of the low expression level of CAR and RGD-binding integrins in human T cells.

Next, we analyzed if transduction by retargeted vectors can be inhibited by adding a vast excess of adapters because of competition effects. We incubated increasing molar ratios of IL-2- and anti-CD28-adapter to knob with iRFP-encoding HAdV-C5 prior to addition of the mixture to pre-activated PBMCs (Figure 3B). Receptor-specific interaction was confirmed by reduced T cell transduction due to an oversaturation of available receptors on the cell membrane. Transduction efficiency dropped from 37% (1:100 knob/adapter) to 12% (1:4,000) using an excess of IL-2 adapters, while a reduction from 21% (1:100) to 4% (1:4,000) was measured by excess of anti-CD28 adapters.

To determine target-specific transduction by anti-CD3 adapters, we generated a CD3-deficient (ΔCD3) Jurkat T cell line by Cas9-mediated knockout (Figure S4). The parental Jurkat cells were mixed with ΔCD3 Jurkat cells and transduced using iRFP-encoding HAdV-C5 that are either untargeted or retargeted with an anti-CD3 adapter (Figures 3C and S5). As expected, untargeted vectors did not show a preferential transduction of CD3-positive (6%–10% of all cells) compared with CD3-negative (5%–10% of all cells) Jurkat cells (Figure 3C). In contrast, HAdV-C5 retargeted with anti-CD3 adapters favored transduction of $CD3^+$ cells: anti-CD3 retargeted vectors transduced 80%–88% of $CD3^+$ Jurkat cells (32%–35% of all cells), whereas the transduction efficiency in $CD3^-$ Jurkat cells remained similar to U/AdV, with 7%–13% of all cells being $CD3^-$ and $iRFP^+$ (Figure 3C).

Having shown receptor-specific transduction using single adapters, we investigated if Comb.R/AdVs exhibit T cell-directed transduction in a mixed cell population. We found strong iRFP expression in T cells within a population of pre-activated PBMCs upon transduction, whereas only minor transduction events but no population shift was observed in $CD3^-$ cells (Figure 3D). This target specificity also remained if we applied our previously described adenoviral protein-shield (Figure S6), although a reduction of transduction efficiency is observed similar as reported for human cancer cells.[29,30]

Retargeting adapters are compatible with high-capacity adenoviral vectors

After demonstrating T cell-directed transduction by using a combination of CD3-, CD28-, and IL-2R-targeted adapters, we investigated the compatibility with high-capacity adenoviral vectors (HC-HAdV) to enable the full potential of adenoviral vectors. A major benefit of HC-HAdV is the packaging capacity of up to 37 kb while lacking any viral genes, thereby making it intrinsically impossible to contain residual expression of viral proteins and reduce recognition through MHC class I presentation.[39,40] To verify the compatibility of our adapters, we generated HC-HAdV and compared their transduction efficiency to a first-generation adenoviral vector (FG-HAdV). Calculations of adapter/fiber knob ratios were performed using optically determined viral particles (vp). However, to achieve a comparable multiplicity of infection (MOI), genomic particles per cell (gp/cell) were used for titrations (Figure S7). Although different viral preparations are notoriously difficult to compare, our data suggest that our adapter combination efficiently mediates transduction of activated T lymphocytes, independent of the adenoviral vector type (FG-HAdV or HC-HAdV).

Retargeted vectors do not cause activation-induced cell death

To achieve broad applicability of our platform, we investigated signals of overstimulation which could cause issues for further applications. CD3/CD28-mediated overstimulation has been reported to promote apoptosis via activation-induced cell death (AICD), potentially limiting application because of safety concerns.[41,42] To assess if adapter-retargeted vectors induce a rapid decline of cell numbers, activated PBMCs were transduced with first-generation untargeted HAdV-C5, Comb.R/AdVs, or vectors individually bound to either anti-CD3, anti-CD28, IL-2 or non-binding adapters. We compared corresponding growth curves using a mock transduction as an additional control (Figure 4A). Neither one of the individual constructs nor their combination induced a rapid decline in cell numbers or halted growth. Furthermore, we measured IFN-γ secretion 48 h post-transduction and observed only minor induction of IFN-γ after Comb.R/AdV transduction, which was non-significant compared with controls (Figure 4B). Although an increase of IFN-γ was observed using anti-CD3 as the only retargeting adapter, this effect was reduced by using Comb.R/AdV in pre-activated PBMCs presumably because of the lower anti-CD3 concentration contained in the combinatorial adapter design.

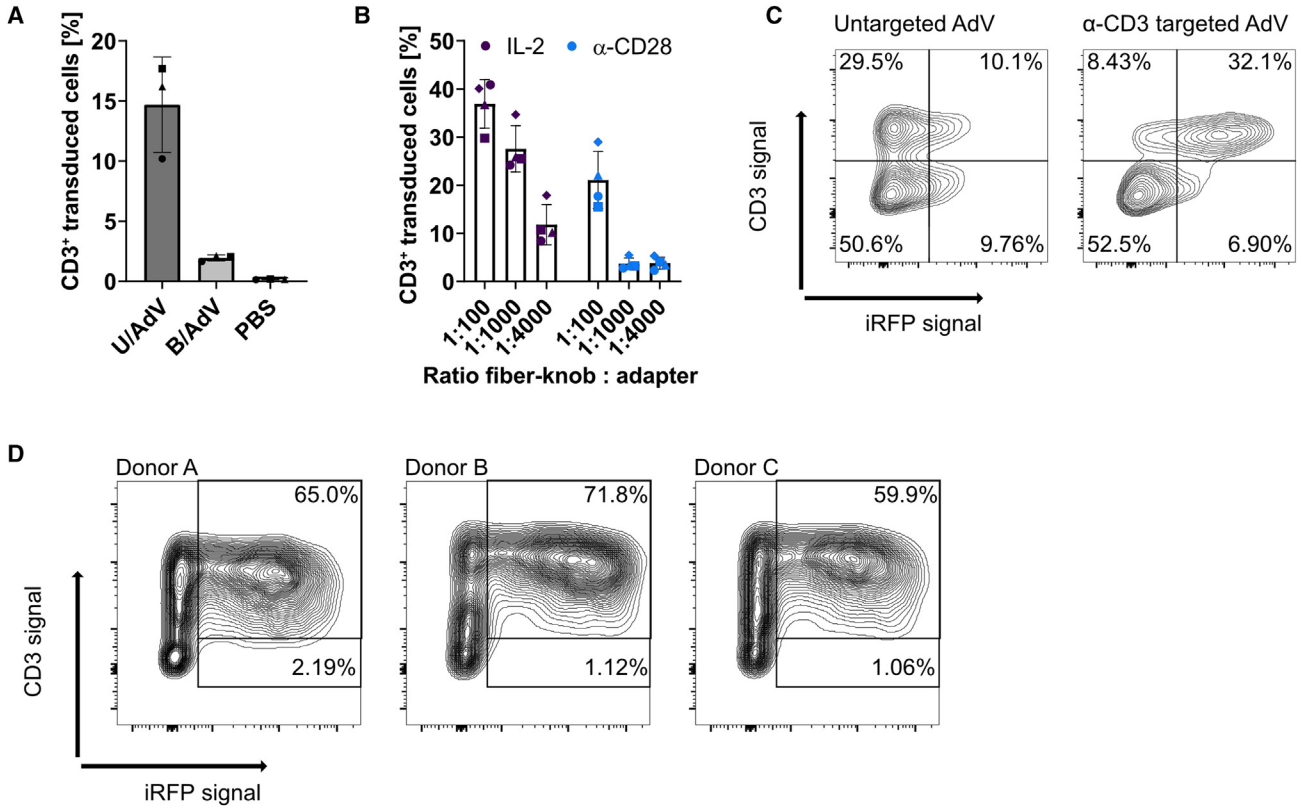

Figure 3. Receptor specificity of adapter-mediated transduction

(A) Quantification of human T cells expressing iRFP after incubation of pre-activated PBMCs with untargeted vectors (U/AdV), vectors coated with non-binding adapters (B/AdV), or PBS (n = 3). (B) Competition assay on pre-activated PBMCs. Transduction efficiency measured by flow cytometry by increasing adapter/knob ratios using IL-2-containing (violet) or α-CD28 scFv-containing (blue) adapters (n = 4). (C) Transduction experiment using HAdV-C5 vectors coated with α-CD3 scFv-containing adapters (α-CD3-targeted vector) or without adapter coating (untargeted vector). Vectors were incubated with a mixture of CD3 knockout Jurkat T cells and their parental cell line. Representative data are shown of three transductions, and two additional replicates are depicted in Figure S5 (n = 3). (D) T cell-directed transduction in different donors. PBMCs stained for CD3 after transduction using Comb.R/AdV. PBMCs were pre-activated and transduced using retargeting vectors covered with a 1:1:1 ratio of IL-2, α-CD3 scFv, and α-CD28 scFv containing adapters (Comb.R/AdV) (n = 3). Individual panels represent single donors. Bar graphs represent mean ± SD.

Retargeted and shielded vectors transduce human T cells *in vivo* in PBMC-reconstituted NSG mice

After confirming efficient targeting and transduction *in vitro* without observing indications of toxic side effects, we applied our adapter strategy *in vivo*. Importantly, to avoid severe side effects caused by vector sequestration into the liver, we included our previously described adenoviral protein shield[29] for all *in vivo* experiments. The trimeric shield protein is based on a hexon-binding humanized scFv derived from the neutralizing hexon-antibody 9C12. It has previously been shown to significantly reduce sequestration into the liver, making it a promising tool for *in vivo* applications. Even though shielded HAdV-C5 somewhat reduces transduction efficiency in T cells (Figure S6), previous applications of this shield demonstrated very favorable target-to-liver ratios.[29]

To investigate *in vivo* transduction with simultaneously retargeted and shielded HAdV-C5 vectors (Comb.R.S/AdV), we intraperitoneally (i.p.) injected 4×10^6 pre-activated PBMCs into NSG (NOD.Cg-*Prkdc*^{scid} *Il2rg*^{tm1Wjl}/SzJ) mice followed by 8×10^{10} Comb.R.S/AdV viral particles, untargeted but shielded viral particles, or PBS (Figure 5A). Forty-eight hours after injection, cells were retrieved and analyzed using flow cytometry.

Using Comb.R.S/AdVs, we observed substantial T cell transduction *in vivo*, yielding reporter expression in 11% of all T cells, including successful transduction of both CD4$^+$ and CD8$^+$ T cells at similar rates (Figure 5B). Ten percent of CD4$^+$ T cells expressed the reporter protein, with CD4$^+$ T cells accounting for 60%–75% of all CD3$^+$ T cells, while 14% of CD8$^+$ T cells were transduced. Even though transduction of CD19$^+$ B cells was observed (6%), transduction of CD3$^-$CD56$^+$ natural killer cells and CD3$^-$CD19$^-$CD56$^-$CD11c$^+$ monocyte uptake remained low (3% and 2%, respectively) (Figure 5C). In contrast, in mice treated with untargeted and shielded vector (U.S/AdV), only 3% of all T cells were transduced with similar rates in B cells (2%), natural killer cells (2%), and monocytes (3%), thus not indicating a T cell-directed transduction (Figure 5C).

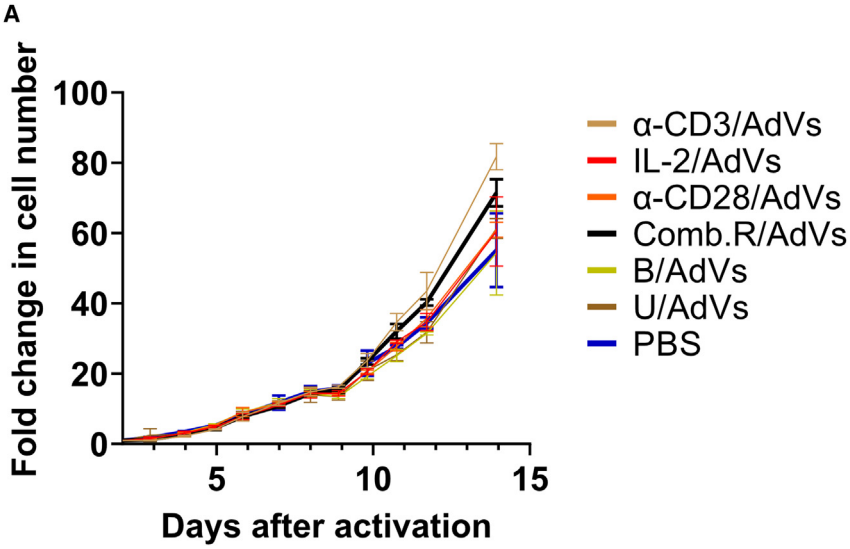

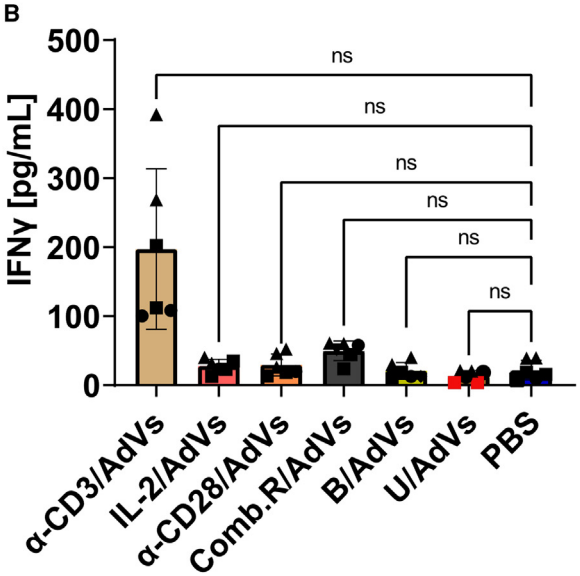

Figure 4. No toxic overstimulation was observed after transduction via different adapters or a combination thereof

(A) Pre-activated PBMCs were transduced using different adapter constructs, combined adapters in 1:1:1 ratio (Comb.R/AdVs), no adapters (untargeted vectors U/AdVs), or PBS. Cell growth was monitored by semi-automated microscopy until 14 days after activation. The experiment was performed on PBMCs from three independent donors (n = 3 independent donors counted 4 times for each time point). (B) IFN-γ secretion 48 h after transduction using HAdV-C5 previously incubated with anti-CD3 adapters, IL-2 adapters, anti-CD28 adapters, a combination of adapters using a 1:1:1 ratio (Comb.R/AdVs), untargeted HAdV-C5 without the addition of adapters (U/AdVs), or PBS. Red marked symbols refer to signal below detection limit (n = 3 independent donors; a-CD3/AdV to PBS, ns, p = 0.2419; IL-2/AdV to PBS, ns, p = 0.888; a-CD28/AdV to PBS, ns, p = 0.5416; Comb.R/AdV to PBS, ns, p = 0.2213; B/AdV to PBS, ns, p = 0.9943; U/AdV to PBS, ns, p = 0.7537; determined using one-way ANOVA with Dunnett's test for multiple comparisons). Individual symbols represent single donors, and repeated transductions using the same donor are indicated by addition of the same symbol. Bar graphs represent mean ± SD.

As certain *in vivo* applications will require transduction of non-activated T cells, NSG mice were also i.p. injected with 4×10^6 viable non-stimulated PBMCs followed by i.p. injection of either 8×10^{10} fully retargeted and shielded viral particles (Comb.R.S/AdVs) or PBS. Forty-eight hours after injection, 3% of all $CD3^+$ T cells expressed the reporter protein in mice receiving the corresponding vector, leading to 3% and 5% positive transduced $CD4^+$ and $CD8^+$ T cells, respectively (Figure 5D).

Successful *in vivo* transduction of T cells in humanized mice using Comb.R.S/AdVs

Encouraged by the successful *in vivo* transduction of T cells in the PBMC NSG model, we moved to a clinically more relevant model. For this purpose, we used NSG mice reconstituted with human $CD34^+$ hematopoietic progenitor cells leading to functional human immune system components including human T cells.[43,44] Forty-eight hours after intravenous (i.v.) injection of 1×10^{11} Comb.R.S/AdVs, spleen, and blood were harvested and analyzed using flow cytometry (Figure 6A). In animals receiving Comb.R.S/AdVs, we detected 0.3% transduced T cells, which is modestly but significantly above the background of 0.1% in the PBS control (Figure 6B). Furthermore, using flow cytometry analysis, no significant transduction of B cells could be detected (Figure 6C), suggesting successful T cell-directed transduction consistent with our previous *in vitro* and *in vivo* data.

To confirm transduction rates and distinguish them from subtle changes in autofluorescence, we used single-cell population qPCR as an orthogonal detection method (Figure 6D). In contrast to the PBS control, the viral gene encoding the hexon protein was detected in both fluorescence-activated cell sorting (FACS)-sorted T and B lymphocytes harvested from vector-treated animals. We detected 0.003 hexon genes per $CD3^+$ T cell, which corresponds to one adenoviral genome per transduced T cell, on the basis of our flow cytometry data of 0.3% reporter-positive $CD3^+$ T cells. Although no B cell transduction was detected by flow cytometry, the more sensitive qPCR analysis discovered low amounts of adenoviral genomes in B cells,

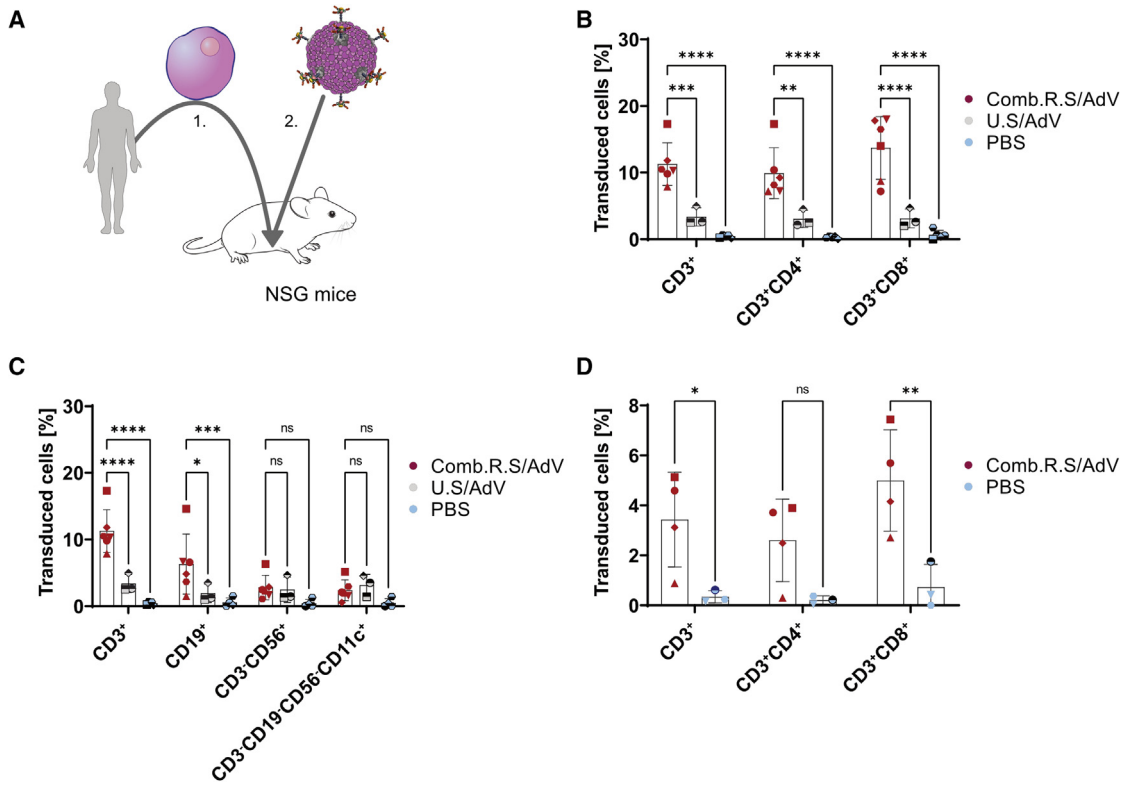

Figure 5. Transduction of T cells by Comb.R.S/AdV in NSG mice

(A) Schematic outline of the mouse experiments by injection of 4×10^6 PBMCs followed by 8×10^{10} vp of retargeted and shielded HAdV, using an adapter combination (Comb.R.S/AdV), or untargeted but shielded vectors without adapters (U.S/AdV). (B) Quantification of transduced cells (percentage) in human T cell subtypes using pre-activated PBMC with Comb.R.S/AdV (n = 6; data pooled from two donors), U.S/AdV (n = 3), or PBS (n = 4) (**p = 0.0024, ***p = 0.0005, and ****p < 0.0001, determined using two-way ANOVA with Šidák multiple-comparisons test). (C) Quantification of transduced cells (percentage) in different cell subtypes using pre-activated PBMC with Comb.R.S/AdV (n = 6; data pooled from two donors), U.S/AdV (n = 3), or PBS (n = 4) (ns, p > 0.05, *p = 0.0163, ***p = 0.0006, and ****p < 0.0001, determined using two-way ANOVA with Šidák multiple-comparisons test). (D) Quantification of transduced cells (percentage) in human T cell subtypes using non-pre-activated PBMCs and Comb.R.S/AdV (n = 4) or PBS (n = 3) *p = 0.0467 and (**p = 0.0057; ns, p = 0.1516; determined using two-way ANOVA with Šidák multiple-comparisons test). Parental cells represent all living human $CD45^+$ and mouse $CD45^-$ cells. Individual symbols represent single mice. Data are shown as mean ± SD.

while the rate was significantly lower (0.001 viral genomes per B cell). Taken together, our data confirm successful *in vivo* transduction of human T cells by HAdV-C5 vectors in a clinically relevant humanized mouse model.

DISCUSSION

Our results provide a proof of concept for a modular adapter system to successfully redirect shielded HAdV-C5 to human T cells. We achieved T cell-directed transduction *in vitro* and *in vivo* with and without prior stimulation using a combination of retargeting adapters. These adapters can be applied with any adenovirus serotype 5 by simply incubating it with our adapters for 1 h, making this approach rather accessible. The retargeted HAdV-C5 presented here elicits increased expression of the early activation marker CD69, suggesting direct activation of T cells. The wide usage and safety of HAdV-C5-based vectors in various clinical trials, and more recently in vaccination strategies for severe acute respiratory syndrome coronavirus 2 (SARS-CoV-2) vaccines, established a foundation for numerous scientific and clinical applications. By generating modular adapters directly applicable for all existing HAdV-C5 vectors, the technology described here can be readily adopted by current research strategies, potentially improving efficacy, potency, and safety of various applications.

The generation of engineered T cells using HC-AdVs is attractive for various reasons. Using non-integrative HAdVs circumvents unpredictable long-term effects which might be caused by semi-specific integration or other viral systems, and it therefore affords additional freedom in payload design and application strategy, combined with the large cargo size of a helper-dependent virus. Nevertheless, the episomal localization of adenoviral delivered constructs can be used for transgene expression for up to several months, as shown in mice and non-human primates.[45,46] If integration is desired, HC-AdV vectors have also been shown to be suitable as a single agent to deliver Cas9-related technologies, including the donor DNA for facultative site-specific integrations and deletions, resulting in

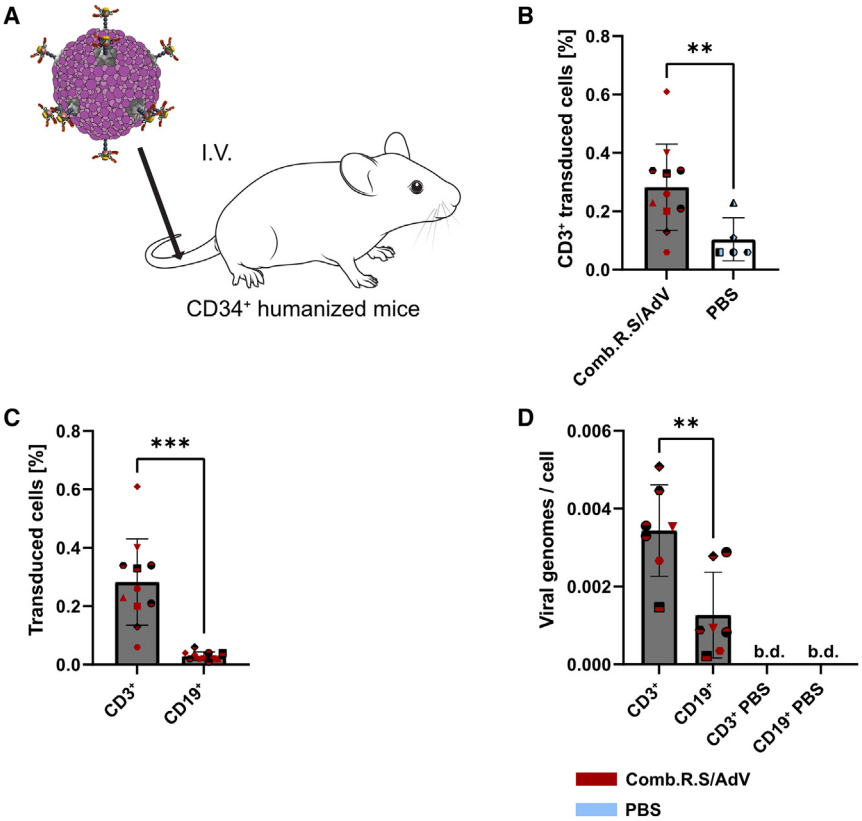

Figure 6. Successful *in vivo* transduction of T cells in humanized mice using Comb.R.S/AdV vectors

(A) Schematic outline of the experiment: mice reconstituted with CD34⁺ hematopoietic progenitor cells from two human fetal liver donors were injected with 1×10^{11} Comb.R.S/AdV vp (n = 11) or PBS (n = 5). (B) **p = 0.062 (determined using unpaired two tailed t test) and (C) quantification of transduced T cells compared with PBS or B cells (CD19⁺). Cells were harvested from both blood and spleen, and percentage of transduction is reported from the total observed cell number (***p = 0.0002, determined using a two-tailed paired t test). Data are pooled from two independent donor-cohorts. (D) qPCR analysis of HAdV-C5 hexon genomes in sorted CD3⁺ or CD19⁺ cells harvested from the spleen (n = 7). Samples from PBS injections were below the detection limit (b.d.). Parental cells represent all living human CD45⁺ and mouse CD45⁻ cells; each symbol represents the average of a technical duplicate (**p = 0.0014, determined using paired two-tailed t test). Data are shown as mean ± SD.

maximal flexibility for cargo design.[16] Furthermore, the large capacity has been reported to be able to express multiple therapeutic transgenes delivered by a single vector.[15,47] Altogether, this places HAdV retargeted to T cells in a pivotal role for complex applications, including synthetics networks or additive therapeutic transgenes.

We believe that those aspects could directly be implemented in T cells using current standard *ex vivo* applications with our retargeting adapters. Also, targeted transduction of human T cells *in vivo* could be further developed as an avenue to an off-the-shelf cell therapy, addressing the enormous burden brought by the effort, cost, and complexity necessary with current *ex vivo* applications of CAR-T therapy. Although transduction percentages in CD34⁺ reconstituted humanized mice were modest and therapeutic effects of relevant transgenes still have to be investigated, the amount of transduced T cell can be put in perspective with current FDA-approved CAR-T doses. Tisagenlecleucel (Kymriah) is an anti-CD19 CAR-T therapy with a current recommended dose for adult patients of 0.6×10^8 to 6.0×10^8 CAR-positive cells.[48] As the number of T cells in a human is estimated at approximately 3×10^{11},[49] this results in a dose of 0.02% to 0.2% of CAR-T cells with respect to all human T cells.

Viral vector applications always bear a risk for hepatotoxicity, which will have to be investigated in the context of our T cell targeting adapters. However, others have already monitored alanine transaminase (ALT) levels after i.v. administration of 1×10^{11} vp HAdV-C5 and analyzed these levels in comparison with the amount of AAV-8 necessary to achieve similar therapeutic efficacy.[50] Although efficacy was higher using first-generation HAdV-C5 compared with AAV-8, ALT levels were similar with both vectors and decreased to baseline after 10 days. Furthermore, adapter-retargeted and shielded HAdV-C5 have been described to reduce liver transduction drastically, compared with untargeted HAdV-C5,[29] potentially widening the window of possible doses. Although toxicity and safety studies will have to be conducted in detail, the previously described data suggest feasibility of T cell-directed transduction for various possible applications.

Our data on pre-activated T cell transduction through untargeted adenoviral vectors suggest that there is a potential interaction of HAdV-C5 with human T cells through the fiber-knob. This interaction can effectively be inhibited by using a blocking adapter, known from crystal structures to sterically compete with CAR, but possibly also competing with another surface molecule which has not yet been identified.[26,27] Even though HAdV infections of T cells with untargeted vectors were difficult to achieve *in vitro*, adenoviral genomes are found in T lymphocytes from tonsils and colon, raising questions about the role of T cell infection in HAdV persistence, which causes high mortality in immunosuppressed children.[51–54]

We have shown here proof-of-concept experiments of human T cell transduction in different models, however, future studies will be required to exploit its potential as a scientific tool or for clinical applications. In-depth analysis of T cell subtype and biodistribution studies should be conducted to use the technology and identify the best suited applications, and the efficacy necessary for desired applications still

must be determined and presumably improved. We presume that the lower transduction in the $CD34^+$ reconstituted humanized mouse model is due to the lower abundance of activated T cells compared with human donor PBMCs. Furthermore, the $CD34^+$ fetal cells used for engraftment do not reconstitute similar levels of memory and primed T cells present in healthy human adults. In addition, the sterile environment of a mouse facility cannot directly be compared with the environmental and microbial exposures of an average adult. Because of this, we propose further studies for *in vivo* application especially in models where inflamed and therefore activated T cells are in high abundance. Nevertheless, our results demonstrate the potential of a broadly applicable platform capable of T cell-directed delivery with a large single vector (up to 37 kb) to address current limitations of *in vivo* application and *ex vivo* payload design in T cell engineering.

MATERIALS AND METHODS

Expression and purification of retargeting adapters

The trimeric adapters were cloned into the mammalian expression plasmid pcDNA3.1. The adapter contained an N-terminal HSA leader peptide, a His_6- and FLAG-tag followed by a 3C cleavage site. The retargeting domain is flanked by a BamHI and an HindIII site for ready exchange of the domain. The adapters were expressed and constructed as previously reported.[28] Following seven days of expression, supernatants were dialyzed against 1,000 volumes of PBS (pH 7.4) using dialysis tubes with a molecular weight cut-off (MWCO) of 12–14 kDa at 4°C. During 24 h, the buffer was exchanged four times at a ratio of 1:10. Dialyzed supernatants were applied to 2.5 mL equilibrated nickel-nitrilotriacetic acid (Ni-NTA) resin (Thermo Fisher Scientific) in PD-10 columns (Merck Millipore). All columns were washed with 5 column volumes of 20 mM imidazole, 10% glycerol, and PBS (pH 8.0) and then additionally with 5 column volumes of 500 mM NaCl and 50 mM Tris HCl (pH 8.0). The samples were then eluted with 0.7 M imidazole in PBS (pH 8.0), followed by 3C (GenScript) cleavage of the tags during dialysis against 100 volumes of 20 mM HEPES (pH 7.4). An additional purification step included an anion exchange chromatography using a Mono Q column (GE Healthcare). Purified protein was dialyzed four times for 24 h against 100 volumes of endotoxin-free PBS (Merck Millipore) and then snap-frozen in liquid nitrogen and stored at −80°C until use.

Viral vector generation

Replication-deficient first-generation HAdV-$C5^{HVR7}$ contain an E1/E3 deletion and 4 mutations in the hyper variable region 7 (HVR7) of the hexon protein (I421G, T423N, E424S, and L426Y). Variants were either generated as previously described[29] or ordered from Vector Biolabs. Briefly, HEK293 cells were transfected with the viral reporter plasmid and cell lysate was used for further amplification. As transgenes, iRFP or tdTomato were encoded in expression cassettes containing a constitutive CMV promoter. The high-capacity adenovirus is devoid of all adenoviral genes and harbors the identical 4 mutations in the hexon protein as the first-generation virus. The HC-AdV was produced as described by Brücher et al.,[15] encoding eGFP as a transgene under the control of the constitutive EF1-α promoter. In short, the cell line 116 was transfected with the reporter plasmid containing the HAdV-C5 packaging signal and co-transduced with helper virus HAdV-$C5^{HVR7}$ for replication. For both, first-generation HAdV-C5 and HC-AdV, purification was performed via two CsCl gradients at 250,000 × *g*.

Cell lines and human tissue and blood samples

Jurkat E6 cells were obtained from ATCC and maintained in R10 Medium (RPMI 1640, 10% fetal calf serum [FCS], 1% penicillin-streptomycin) at a density of 0.5×10^6 to 2×10^6 cells/mL. The ethical approval for the use of human fetal liver tissue (from Advanced Bioscience Resources) as well as peripheral blood samples of healthy adult volunteers was obtained from the cantonal ethical committee of Zurich, Switzerland (protocol KEK-StV-Nr.19/08). Leukocyte concentrate from human donors was acquired from Blutspende Zurich, Zurich, Switzerland. After Ficoll-Paque (GE Healthcare) gradient separation, donor cells were aliquoted and frozen to be thawed before each assay. To use pre-activated cells, thawed PBMCs were cultured in R10 at 1×10^6 cells/mL and supplemented with a 1:1 ratio of Dynabeads Human T-Expander CD3/CD28 (Thermo Fisher Scientific) and 200 IU/mL human IL-2 (PeproTech) and incubated for 24 h. Afterwards, magnetic beads were removed from activated cells using a magnetic strip and washed twice with R10. Non-pre-activated cells were cultured in R10 supplemented with 50 IU/mL of IL-2.

In vitro retargeting assays

PBMCs were thawed 24 h prior to transduction and taken in culture. Cells were distributed in round-bottom 96-well plates with 5×10^4 cells/well in 100 μL R10. Adenoviral vectors were incubated for 1 h at 4°C with retargeting adapters containing an α-CD3 scFv and/or IL-2 and/or α-CD28 scFv (termed "retargeted"), or a blocking adapter containing the consensus DARPin E2_5 (termed "non-binding adapter"). Optionally, the previously described shield[29] was added (termed "shielded"). As a control, adenoviral vectors without adapters were incubated with PBS (termed "untargeted vector"). The molar ratio of total retargeting adapter to fiber-knob was 32.5:1 and for the shield 5:1 per hexon subunit. Twenty thousand optical viral particles were used per cell. Viral particle-containing supernatants were removed 16 h after transduction and replaced by fresh culture medium. The activity of the transduced transgene was determined by flow cytometry 48 h after transduction.

Specificity assays

For competition assays, the procedure followed the *in vitro* retargeting assays, however, ratios of adapter to knob were increased in the steps indicated. For CD3 specificity, CD3 knockout cells were prepared. For this purpose, 2×10^5 Jurkat T cells were electroporated in OptiMEM with a total of 90 pmol ribonucleoprotein (30 pmol CD3δ RNP, 30 pmol CD3ε RNP, 30 pmol CD3γ RNP) in one well of a 16-well strip (catalog #V4XP-3032; Lonza) with the CL-120 pulse using the 4D Nucleofector (Lonza). SpCas9 (catalog #1081059; IDT), crRNA, and trRNA (catalog #1072533; IDT) were ordered from IDT. Electroporated Jurkat T cells were expanded for 10 days. Cells were subsequently purified by removing $CD3^+$ cells by MACS (catalog #130-050-101; Miltenyi Biotec) using the autoMACS machine

(Miltenyi Biotec). The following crRNA sequences were used to delete functional CD3 expression: CD3δ: AAACGCAUCCUGGACCCA CG CD3ε: AGAUAAAAGUUCGCAUCUUC CD3γ: UACACUGA UACAUCCCUCGA.

Cytokine detection

IFN-γ expression was detected in 384-well plates using Human ELISA Kits (KHC4021; Invitrogen), following the manufacturer's instructions. Volumes were adjusted accordingly. Absorbance measurements were performed using an Infinite M1000 instrument, following the manufacturer's instructions.

Growth measurements

PBMCs were activated 24 h prior to transduction as described above for the *in vitro* retargeting assays. Media were replaced with R10 containing 50 IU/mL IL-2 16 h after transduction and replaced with fresh R10 supplemented with 50 IU/mL IL-2 every second day. The number of total cells was counted daily using an Arthur cell counter, including all cells between 5 and 15 μm in diameter to the count. Three independent donors were transduced and counted four times per day.

Animal experiments

NOD-*scid* γ_c^{null} (NSG) mice were obtained from The Jackson Laboratory and bred and maintained under specific pathogen-free conditions at the Institute of Experimental Immunology, University of Zurich. Both male and female mice were used for experiments at the age of 12–15 weeks. Four million viable PBMCs, with or without 24 h pre-stimulus with CD3/CD28 Dynabeads (Thermo Fisher Scientific), were injected intraperitoneally followed by 8×10^{10} HAdV-C5^{HVR7} vector particles. These first-generation HAdV-C5^{HVR7} were incubated with IL-2, anti-CD28, and anti-CD3 adapters, as well as previously described hexon-covering shield[29] for 2 h at 4°C (fully retargeted and shielded) or only with the hexon-covering shield (untargeted). Molar ratios of adapters and shield were the same as stated for the *in vitro* targeting assays. Forty-eight hours after injection, cells were harvested by intraperitoneal lavage with 10 mL of PBS. For experiments with humanized mice, the reconstitution of newborn NSG mice with human immune system components was performed as previously described.[43] Before the start of subsequent experiments, the level of human immune cell reconstitution was checked in blood by flow cytometry. Fully retargeted and shielded first-generation HAdV-C5^{HVR7} were injected intravenously. Mice were sacrificed 48 h after injection and blood and spleen were harvested. The respective animal protocol was approved by the veterinary office of the canton of Zurich, Switzerland.

Flow cytometry

For *in vitro* assays cells were centrifuged at 750 × *g* for 5 min and resuspended in PBS containing 1% BSA and 0.05% azide as well as all used antibodies. Cells were then kept at 4°C in the dark for 30 min and washed twice with PBS. Cells were then resuspended in PBS containing 2% paraformaldehyde (PFA) and fixed for 15 min at room temperature. Remaining PFA was then quenched by adding PBS containing 1% BSA and 0.05% azide with a volume of 5 times the fixation volume. For *in vivo* analysis, erythrocytes in blood samples were lysed three times with NH_4Cl. Spleens were mechanically mashed through a 70 μm cell strainer before isolation of lymphocytes using density gradient centrifugation. Bone marrow was extracted by centrifugation of bones that were cut open at one end and directly used for antibody labeling. Cells were stained with the appropriate amount of antibodies for 20 min at 4°C in PBS and fixed with PBS plus 2% PFA for 30 min at 4°C. Samples were analyzed using a BD LSRFortessa flow cytometer (BD Biosciences). The following antibodies were used: CD3 (PerCP-Cy5.5/BioLegend/UCHT1/300429), CD4 (Pacific Blue/BioLegend/RPA-T4/#300521), CD8 (Brilliant Violet 650/BioLegend/SK1/#344730), hCD45 (Qdot 605 BioLegend/HI30/#304042), mCD45 (APC-Cy7/BioLegend/30-F11/#103116), CD11c (PE-Cy7/BD/B-ly6/#561356), CD28 (Pe-Cy7/Invitrogen/CD28.2/#25-0289-42), CD19 (Qdot800/BioLegend/HIB19/#302239), CD56 (Qdot 655/Biolegend/NCAM/#318343), CD69 (FITC/Invitrogen/CH/4/#MHCD6901), live dead stain (Zombie Aqua/BioLegend/#423101).

Fluorescence-activated single-cell sorting

Lymphocytes isolated from the spleen were stained for anti-human CD19, anti-human CD45, anti-human CD3, and anti-murine CD45 as described. One hundred thousand $CD3^+$ and 100,000 $CD19^+$ events were sorted using a FACSAria III cell sorter using the 100 μm nozzle and BD FACS Diva Software (BD Biosciences). Purity of the samples was confirmed after the sort by re-analysis.

Quantitative polymerase chain reaction analysis

For *in vitro* measurements, cells were digested using the protein K Arcturus PicoPure® DNA Extraction Kit (Thermo Fisher Scientific), and the digested cell lysate was directly used for qPCR analysis without further DNA purification. For *in vivo* data, viral and cellular genomes were extracted from tissues using the DNeasy Blood & Tissue Kit (69506; Qiagen) following the manufacturer's protocol. DNA amounts were quantified by qPCR with specific primers for hβ2m and adenoviral hexon protein, respectively. To investigate the amount of viral vector genomes, the primers 5′-GAA TAA CAA GTT TAG AAA CCC CAC GGT GG-3′ and 5′-GTT TGA CCT TCG ACA CCT ATT TGA ATA CCC-3′ were used, resulting in a 149-bp-long amplicon. For cellular genomes of human origin, hβ2m 5′-GGA ATT GAT TTG GGA GAG CAT C-3′ and 5′-CAGGTCCTGGCTCTACAATT TACTAA-3′ were used to result in a 79-bp-long amplicon. Specific probes were the following: for the hexon (5′-CGG CGT GCT GGA CAG G-3′) and hβ2m (5′-AGT GTG ACT GGG CAG ATC ATC CAC CTT C-3′). Reactions were performed using PrimeTime Gene Expression Master Mix (105571; IDT) and signals were normalized using dye rhodamine-X (ROX). All qPCR primer and probes were generated with the double-quench technology by IDT. qPCR was performed and analyzed as described previously.[15]

DATA AVAILABILITY

Supplemental data are provided with this paper. All data are also available upon request.

SUPPLEMENTAL INFORMATION

Supplemental information can be found online at https://doi.org/10.1016/j.omtm.2023.02.012.

ACKNOWLEDGMENTS

We would like to thank Urs Greber and Maarit Suomalainen for their technical support and discussions; Danusia Vanoaica for the organization of blood donors and various tasks; Daniel Kirchmeier, Yun Deng, and Lisa Rieble for their help in mice preparation; Seraina Jans for initial work; Fabienne Fischer for statistical advice; and Karina M. Hugentobler for proofreading. We would also like to thank the University of Zurich Cytometry Facility and Laboratory of Animal Services Center. We would like to thank the following funding sources for their support: Cancer Research Switzerland (grants KFS-4371-02-2018 and KFS-5292-02-2021 to O.C.), research fellowship from the German Research Foundation (project 415801544, to M.K.), and Swiss National Science Foundation Sinergia Grant 170929 (to A.P.).

AUTHOR CONTRIBUTIONS

Conceptualization: P.C.F., M.K., S.N.S., O.C., and A.P.; Methodology: P.C.F., M.K., F.W., D.B., and J.K.; Formal Analysis: P.C.F. and M.K.; Investigation, P.C.F., M.K., L.F., J.M., F.W., D.B., J.K., and K.P.H.; Visualization, P.C.F.; Supervision, C.M., O.C., and A.P.; Writing – Original Draft: P.C.F.; Writing – Review & Editing, P.C.F., M.K., F.W., D.B., K.P.H., S.N.S., C.M., O.C., and A.P.; Funding Acquisition, C.M., O.C., and A.P.

DECLARATION OF INTERESTS

A.P. is a cofounder and shareholder and D.B. and S.N.S. are employees and shareholders of Vector BioPharma, which is commercializing this technology. A.P., O.C., P.C.F., and M.K. have filed a patent using the results described here. The other authors declare no conflict of interest.

REFERENCES

1. Lim, W.A., and June, C.H. (2017). The principles of engineering immune cells to treat cancer. Cell *168*, 724–740.
2. Roth, T.L., Puig–Saus, C., Yu, R., Shifrut, E., Carnevale, J., Li, P.J., Hiatt, J., Saco, J., Krystofinski, P., Li, H., et al. (2018). Reprogramming human T cell function and specificity with non-viral genome targeting. Nature *559*, 405–409.
3. Dai, X., Park, J.J., Du, Y., Kim, H.R., Wang, G., Errami, Y., and Chen, S. (2019). One-step generation of modular CAR-T cells with AAV–Cpf1. Nat. Methods *16*, 247–254.
4. Rosenberg, S.A., and Restifo, N.P. (2015). Adoptive cell transfer as personalized immunotherapy for human cancer. Science *348*, 62–68.
5. Leick, M.B., Maus, M.V., and Frigault, M.J. (2021). Clinical perspective: treatment of aggressive B cell lymphomas with FDA-approved CAR-T cell therapies. Mol. Ther. *29*, 433–441.
6. Levine, B.L., Miskin, J., Wonnacott, K., and Keir, C. (2017). Global manufacturing of CAR T cell therapy. Mol. Ther. Methods Clin. Dev. *4*, 92–101.
7. Cornu, T.I., Mussolino, C., and Cathomen, T. (2017). Refining strategies to translate genome editing to the clinic. Nat. Med. *23*, 415–423.
8. Zhao, Y., Zheng, Z., Cohen, C.J., Gattinoni, L., Palmer, D.C., Restifo, N.P., Rosenberg, S.A., and Morgan, R.A. (2006). High-efficiency transfection of primary human and mouse T lymphocytes using RNA electroporation. Mol. Ther. *13*, 151–159.
9. Rurik, J.G., Tombácz, I., Yadegari, A., Méndez Fernández, P.O., Shewale, S.V., Li, L., Kimura, T., Soliman, O.Y., Papp, T.E., Tam, Y.K., et al. (2022). CAR T cells produced in vivo to treat cardiac injury. Science *375*, 91–96.
10. Yu, S., Yi, M., Qin, S., and Wu, K. (2019). Next generation chimeric antigen receptor T cells: safety strategies to overcome toxicity. Mol. Cancer *18*, 125–213.
11. Barry, M.A., Rubin, J.D., and Lu, S.C. (2020). Retargeting adenoviruses for therapeutic applications and vaccines. FEBS Lett. *594*, 1918–1946.
12. Brunetti-Pierri, N., and Ng, P. (2017). Gene therapy with helper-dependent adenoviral vectors: lessons from studies in large animal models. Virus Gene. *53*, 684–691.
13. Hemminki, O., dos Santos, J.M., and Hemminki, A. (2020). Oncolytic viruses for cancer immunotherapy. J. Hematol. Oncol. *13*, 84.
14. Vorburger, S.A., and Hunt, K.K. (2002). Adenoviral gene therapy. Oncol. *7*, 46–59.
15. Brücher, D., Kirchhammer, N., Smith, S.N., Schumacher, J., Schumacher, N., Kolibius, J., Freitag, P.C., Schmid, M., Weiss, F., Keller, C., et al. (2021). iMATCH: an integrated modular assembly system for therapeutic combination high-capacity adenovirus gene therapy. Mol. Ther. Methods Clin. Dev. *20*, 572–586.
16. Palmer, D.J., Turner, D.L., and Ng, P. (2020). A single, All-in-one helper-dependent adenovirus to deliver donor DNA and CRISPR/Cas9 for efficient homology-directed repair. Mol. Ther. Methods Clin. Dev. *17*, 441–447.
17. Greber, U.F., and Flatt, J.W. (2019). Adenovirus entry: from infection to immunity. Annu. Rev. Virol. *6*, 177–197.
18. Hogg, N., Laschinger, M., Giles, K., and McDowall, A. (2003). T-cell integrins: more than just sticking points. J. Cell Sci. *116*, 4695–4705.
19. Bertoni, A., Alabiso, O., Galetto, A.S., and Baldanzi, G. (2018). Integrins in T cell physiology. Int. J. Mol. Sci. *19*, 485.
20. Huang, S., Endo, R.I., and Nemerow, G.R. (1995). Upregulation of integrins alpha v beta 3 and alpha v beta 5 on human monocytes and T lymphocytes facilitates adenovirus-mediated gene delivery. J. Virol. *69*, 2257–2263.
21. Agarwal, P., Gammon, E.A., Sajib, A.M., Sandey, M., and Smith, B.F. (2017). Cell-surface integrins and CAR are both essential for adenovirus type 5 transduction of canine cells of lymphocytic origin. PLoS One *12*, e0169532.
22. Leon, R.P., Hedlund, T., Meech, S.J., Li, S., Schaack, J., Hunger, S.P., Duke, R.C., and DeGregori, J. (1998). Adenoviral-mediated gene transfer in lymphocytes. Proc. Natl. Acad. Sci. USA *95*, 13159–13164.
23. Schroers, R., Hildebrandt, Y., Hasenkamp, J., Glass, B., Lieber, A., Wulf, G., and Piesche, M. (2004). Gene transfer into human T lymphocytes and natural killer cells by Ad5/F35 chimeric adenoviral vectors. Exp. Hematol. *32*, 536–546.
24. Seya, T., Hirano, A., Matsumoto, M., Nomura, M., and Ueda, S. (1999). Human membrane cofactor protein (MCP, CD46): multiple isoforms and functions. Int. J. Biochem. Cell Biol. *31*, 1255–1260.
25. Yu, D., Jin, C., Ramachandran, M., Xu, J., Nilsson, B., Korsgren, O., Le Blanc, K., Uhrbom, L., Forsberg-Nilsson, K., Westermark, B., et al. (2013). Adenovirus serotype 5 vectors with Tat-PTD modified hexon and serotype 35 fiber show greatly enhanced transduction capacity of primary cell cultures. PLoS One *8*, e54952.
26. Dreier, B., Mikheeva, G., Belousova, N., Parizek, P., Boczek, E., Jelesarov, I., Forrer, P., Plückthun, A., and Krasnykh, V. (2011). Her2-specific multivalent adapters confer designed tropism to adenovirus for gene targeting. J. Mol. Biol. *405*, 410–426.
27. Dreier, B., Honegger, A., Hess, C., Nagy-Davidescu, G., Mittl, P.R.E., Grütter, M.G., Belousova, N., Mikheeva, G., Krasnykh, V., and Plückthun, A. (2013). Development of a generic adenovirus delivery system based on structure-guided design of bispecific trimeric DARPin adapters. Proc. Natl. Acad. Sci. USA *110*, E869–E877.
28. Freitag, P.C., Brandl, F., Brücher, D., Weiss, F., Dreier, B., and Plückthun, A. (2022). Modular adapters utilizing binders of different molecular types expand cell-targeting options for adenovirus gene delivery. Bioconjugate Chem. *33*, 1595–1601.
29. Schmid, M., Ernst, P., Honegger, A., Suomalainen, M., Zimmermann, M., Braun, L., Stauffer, S., Thom, C., Dreier, B., Eibauer, M., et al. (2018). Adenoviral vector with shield and adapter increases tumor specificity and escapes liver and immune control. Nat. Commun. *9*, 450.
30. Smith, S.N., Schubert, R., Simic, B., Brücher, D., Schmid, M., Kirk, N., Freitag, P.C., Gradinaru, V., and Plückthun, A. (2021). SHREAD gene therapy platform for

paracrine delivery improves tumor localization and intratumoral effects of a clinical antibody. Proc. Natl. Acad. Sci. USA *118*. e2017925118.

31. Kirchhammer, N., Trefny, M.P., Natoli, M., Brücher, D., Smith, S.N., Werner, F., Koch, V., Schreiner, D., Bartoszek, E., Buchi, M., et al. (2022). NK cells with tissue-resident traits shape response to immunotherapy by inducing adaptive antitumor immunity. Sci. Transl. Med. *14*, eabm9043.

32. Yotnda, P., Onishi, H., Heslop, H.E., Shayakhmetov, D., Lieber, A., Brenner, M., and Davis, A. (2001). Efficient infection of primitive hematopoietic stem cells by modified adenovirus. Gene Ther. *8*, 930–937.

33. Shalaby, M.R., Shepard, H.M., Presta, L., Rodrigues, M.L., Beverley, P.C., Feldmann, M., and Carter, P. (1992). Development of humanized bispecific antibodies reactive with cytotoxic lymphocytes and tumor cells overexpressing the HER2 protooncogene. J. Exp. Med. *175*, 217–225.

34. Zhu, Z., and Carter, P. (1995). Identification of heavy chain residues in a humanized anti-CD3 antibody important for efficient antigen binding and T cell activation. J. Immunol. *155*, 1903–1910.

35. Hanke, T., Trischler, M., and Guntermann, C. (2014). Superagonistic anti-CD28 antibodies. U.S. Patent No. 8,709,414.

36. Li, Y., and Kurlander, R.J. (2010). Comparison of anti-CD3 and anti-CD28-coated beads with soluble anti-CD3 for expanding human T cells: differing impact on CD8 T cell phenotype and responsiveness to restimulation. J. Transl. Med. *8*, 104.

37. Appleman, L.J., Berezovskaya, A., Grass, I., and Boussiotis, V.A. (2000). CD28 costimulation mediates T Cell expansion via IL-2-independent and IL-2-dependent regulation of cell cycle progression. J. Immunol. *164*, 144–151.

38. Binz, H.K., Stumpp, M.T., Forrer, P., Amstutz, P., and Plückthun, A. (2003). Designing repeat proteins: well-expressed, soluble and stable proteins from combinatorial libraries of consensus ankyrin repeat proteins. J. Mol. Biol. *332*, 489–503.

39. Yang, Y., Nunes, F.A., Berencsi, K., Furth, E.E., Gönczöl, E., and Wilson, J.M. (1994). Cellular immunity to viral antigens limits E1-deleted adenoviruses for gene therapy. Proc. Natl. Acad. Sci. USA *91*, 4407–4411.

40. Gao, G.P., Yang, Y., and Wilson, J.M. (1996). Biology of adenovirus vectors with E1 and E4 deletions for liver-directed gene therapy. J. Virol. *70*, 8934–8943.

41. Künkele, A., Johnson, A.J., Rolczynski, L.S., Chang, C.A., Hoglund, V., Kelly-Spratt, K.S., and Jensen, M.C. (2015). Functional tuning of CARs reveals signaling threshold above which CD8+ CTL antitumor potency is attenuated due to cell Fas-FasL-dependent AICD. Cancer Immunol. Res. *3*, 368–379.

42. Green, D.R., Droin, N., and Pinkoski, M. (2003). Activation-induced cell death in T cells. Immunol. Rev. *193*, 70–81.

43. Murer, A., McHugh, D., Caduff, N., Kalchschmidt, J., Barros, M., Zbinden, A., Capaul, R., Niedobitek, G., Allday, M., Chijioke, O., and Münz, C. (2018). EBV persistence without its EBNA3A and 3C oncogenes in vivo. PLoS Pathog. *14*, e1007039.

44. Strowig, T., Gurer, C., Ploss, A., Liu, Y.F., Arrey, F., Sashihara, J., Koo, G., Rice, C.M., Young, J.W., Chadburn, A., et al. (2009). Priming of protective T cell responses against virus-induced tumors in mice with human immune system components. J. Exp. Med. *206*, 1423–1434.

45. Butti, E., Bergami, A., Recchia, A., Brambilla, E., Del Carro, U., Amadio, S., Cattalini, A., Esposito, M., Stornaiuolo, A., Comi, G., et al. (2008). IL4 gene delivery to the CNS recruits regulatory T cells and induces clinical recovery in mouse models of multiple sclerosis. Gene Ther. *15*, 504–515.

46. Unzu, C., Melero, I., Hervás-Stubbs, S., Sampedro, A., Mancheño, U., Morales-Kastresana, A., Serrano-Mendioroz, I., De Salamanca, R.E., Benito, A., and Fontanellas, A. (2015). Helper-dependent adenovirus achieve more efficient and persistent liver transgene expression in non-human primates under immunosuppression. Gene Ther. *22*, 856–865.

47. Rosewell Shaw, A., Porter, C., Biegert, G., Jatta, L., and Suzuki, M. (2022). HydrAd: a helper-dependent adenovirus targeting multiple immune pathways for cancer immunotherapy. Cancers *14*, 2769.

48. Upendra, M. (2022). Biologics License Application (BLA) Clinical Review and Evaluation, STN: 125646/663 (Tisagenlecleucel) (US Food and Drug Administration). https://www.fda.gov/.

49. Jenkins, M.K., Chu, H.H., McLachlan, J.B., and Moon, J.J. (2010). On the composition of the preimmune repertoire of T cells specific for peptide–major histocompatibility complex ligands. Annu. Rev. Immunol. *28*, 275–294.

50. Böck, D., Rothgangl, T., Villiger, L., Schmidheini, L., Matsushita, M., Mathis, N., Ioannidi, E., Rimann, N., Grisch-Chan, H.M., Kreutzer, S., et al. (2022). In vivo prime editing of a metabolic liver disease in mice. Sci. Transl. Med. *14*, eabl9238.

51. Garnett, C.T., Erdman, D., Xu, W., and Gooding, L.R. (2002). Prevalence and quantitation of species C adenovirus DNA in human mucosal lymphocytes. J. Virol. *76*, 10608–10616.

52. Garnett, C.T., Talekar, G., Mahr, J.A., Huang, W., Zhang, Y., Ornelles, D.A., and Gooding, L.R. (2009). Latent species C adenoviruses in human tonsil tissues. J. Virol. *83*, 2417–2428.

53. Kosulin, K., Hoffmann, F., Clauditz, T.S., Wilczak, W., and Dobner, T. (2013). Presence of adenovirus species C in infiltrating lymphocytes of human sarcoma. PLoS One *8*, e63646.

54. Kosulin, K., Geiger, E., Vécsei, A., Huber, W.D., Rauch, M., Brenner, E., Wrba, F., Hammer, K., Innerhofer, A., Pötschger, U., et al. (2016). Persistence and reactivation of human adenoviruses in the gastrointestinal tract. Clin. Microbiol. Infect. *22*. 381.e1–e8.

OMTM, Volume *29*

Supplemental information

Targeted adenovirus-mediated transduction of human T cells *in vitro* and *in vivo*

Patrick C. Freitag, Meike Kaulfuss, Lea Flühler, Juliane Mietz, Fabian Weiss, Dominik Brücher, Jonas Kolibius, K. Patricia Hartmann, Sheena N. Smith, Christian Münz, Obinna Chijioke, and Andreas Plückthun

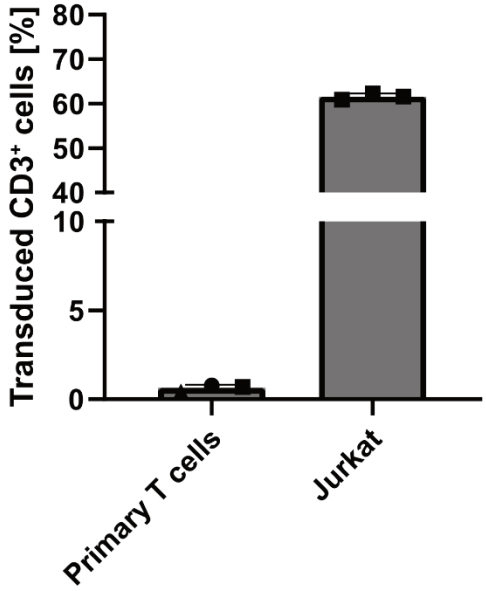

Figure S1. Transduction susceptibility of primary T cells and Jurkat cells with HAdV-C5. 50,000 viable PBMCs or Jurkat cells were transduced with untargeted HAdV-C5 encoding tdTomato. Transduction was quantified by reporter expression via flow cytometry, normalized to the non-transduced control. Symbols represent single donors, repeated transductions using the same donor are indicated by addition of the same symbol. ($n = 3$) Data are shown as mean ± SD.

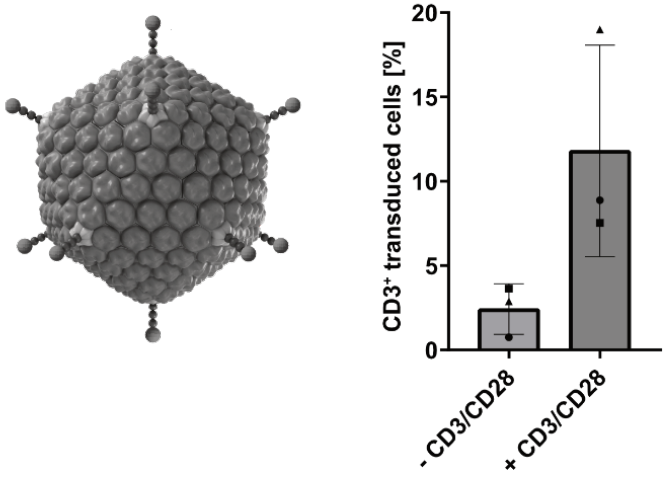

Figure S2. Quantification of human T cells transduced by HAdV-C5 without adapters. PBMCs were either stimulated 24 h prior to transduction (+ CD3/CD28) or transduced without prior activation (– CD3/CD28). ($n = 3$) Data are shown as mean ± SD.

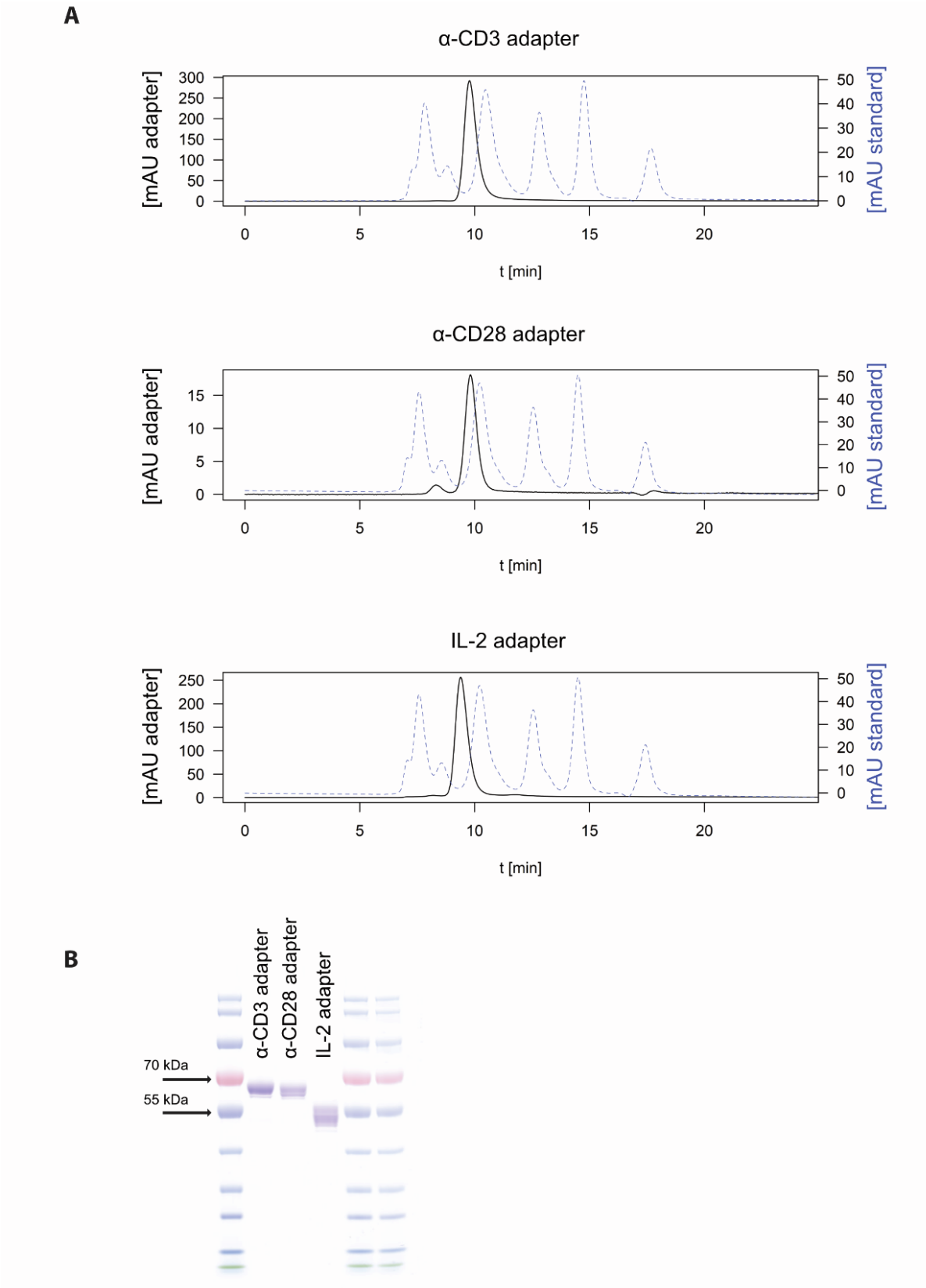

Figure S3. Purity analysis of purified adapter proteins. (*A*) HPLC-SEC analysis of purified adapter proteins compared to a MW standard (AdvanceBio SEC Protein Standard 300A).

mAU: milli absorption unit (*B*) SDS-PAGE analysis of 2 μg purified adapter proteins. Calculated MW values are 55.5 kDa (anti-CD3-adapter), 55.3 kDa (anti-CD28-adapter), and 44.5 kDa (IL-2-adapter).

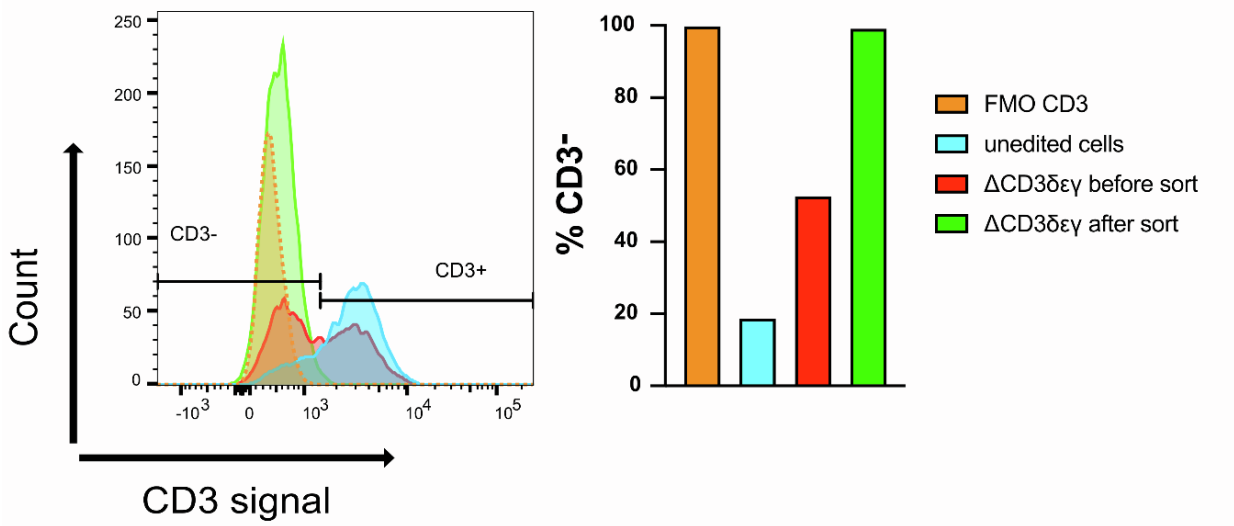

Figure S4. Generation and validation of CD3 knock-out Jurkat cells. Quantification of CD3 expression detected by antibody staining after Cas9-directed knock-out using gRNA directed against the δ-, ε-, and γ-CD3 chain. FMO: Fluorescence minus one (fluorescence signal without CD3 staining), ΔCD3δεγ: Jurkat cells after knock-out using CRISPR/Cas9 ribonucleoprotein electroporation.

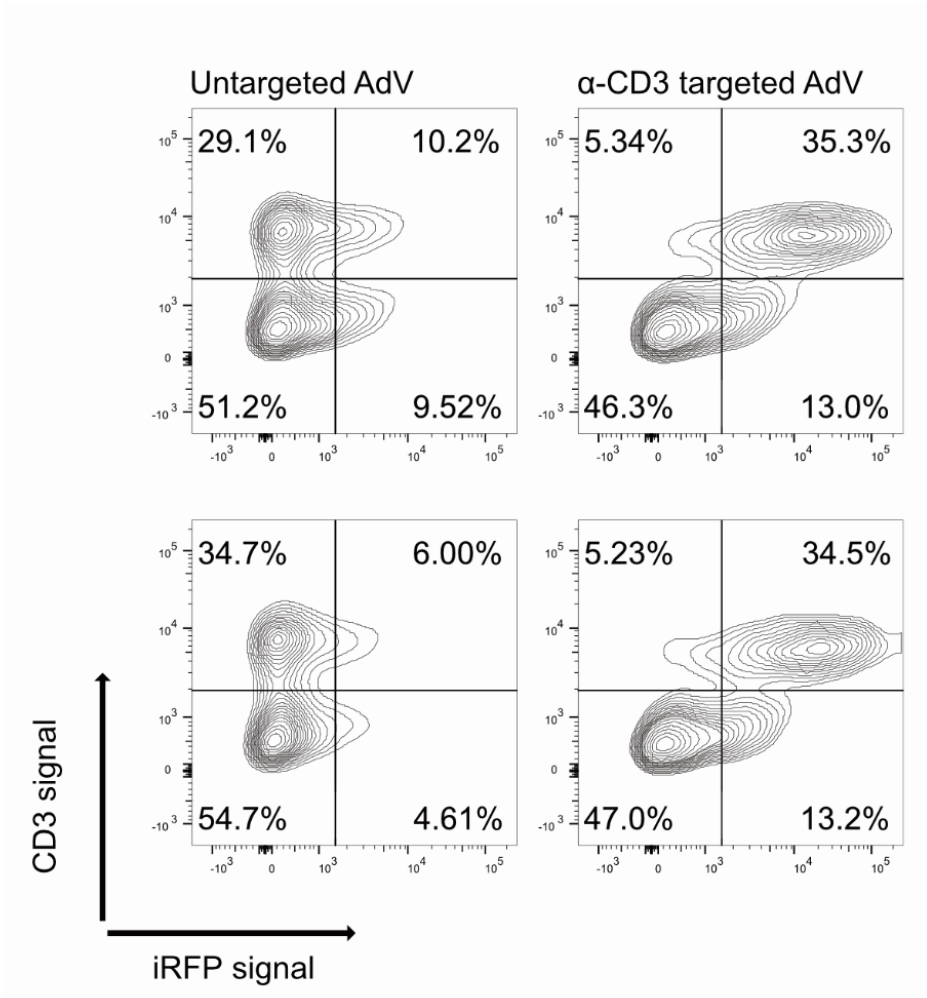

Figure S5. Repetitions of experiment from Fig. 3C with two additional replicates. Experiment was conducted using HAdV-C5 encoding iRFP bound by anti-CD3 adapter. ($n = 3$ one repetition is shown in Fig. 3C)

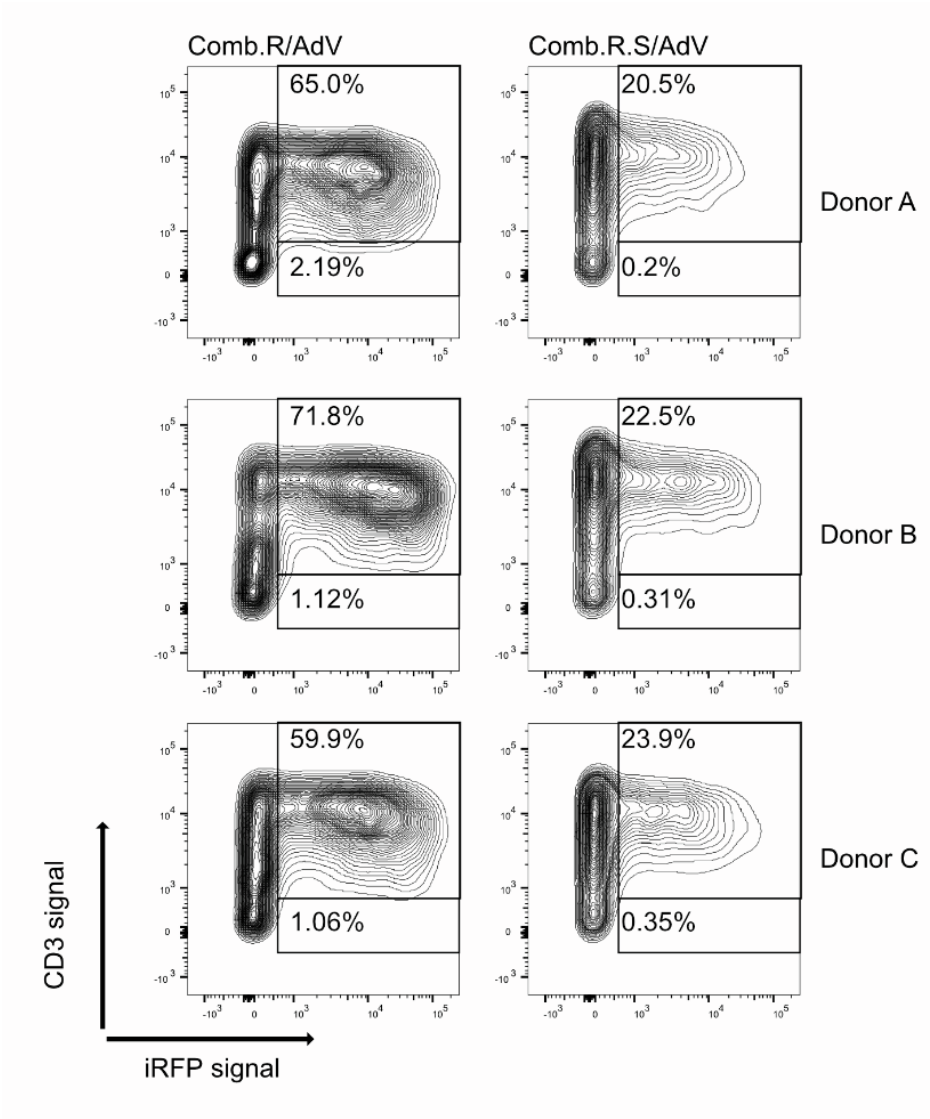

Figure S6. Comparison using shielded or non-shielded retargeted Comb.R/AdB. Transduction efficiency of adapter-retargeted HAdV-C5 with (Comb.R.S/AdV) and without (Comb.R/AdV) protein shield minimizing liver tropism. ($n = 3$)

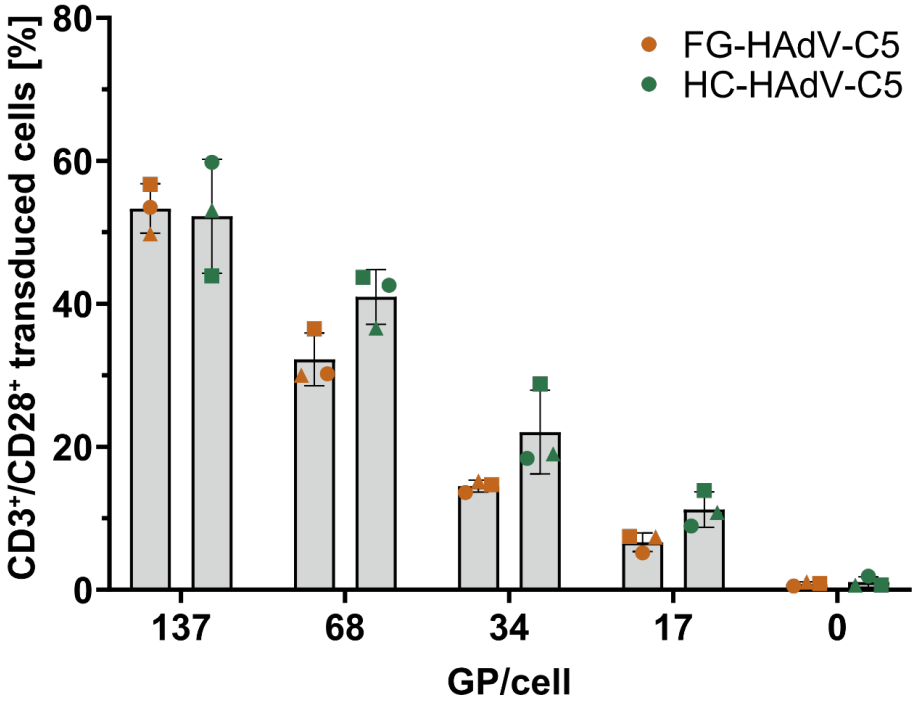

Figure S7. Comb.R/AdV vectors show comparable transduction efficiency with first-generation HAdV-C5 (FG-HAdV-C5) and high-capacity HAdV-C5 (HC-HAdV-C5) vector. Pre-activated PBMCs were incubated with different MOI measured as genomic particles /cell (GP/cell) using Comb.R/AdV FG-HadV-C5 (orange) or HC-AdV-C5 vectors, and transduction efficiency was measured by flow cytometry. Individual symbols represent single donors. ($n = 3$) Bar graphs represent mean ± SD.